



Research Article

Efficiency improvement of semi-evaporative cooling systems through environmental analysis

Vijaykumar Kisan JAVANJAL¹, Subhash GADHAVE^{1,*}, Lalit N. PATIL², Kuldeep A. MAHAJAN³, Swapnil S. JADHAV²

¹Department of Mechanical Engineering, Dr. D. Y. Patil Institute of Technology Pimpri, Pune, 411018, India

²Department of Automation and Robotics, Dr. D. Y. Patil Institute of Technology Pimpri, Pune, 411018, India

³Department of Mechanical Engineering, Modern Education Society's College of Engineering, Pune, 411001, India

ARTICLE INFO

Article history

Received: 20 May 2024

Revised: 03 July 2024

Accepted: 24 July 2024

Keywords:

Air Conditioning; Building Applications; Evaporative Cooler; Heat Pipe; Saturation Efficiency

ABSTRACT

This research delves into semi-evaporative cooling systems, exploring their performance in diverse environments with a focus on air supply, temperature, and humidity. Findings highlight the importance of environmental factors, especially the evaporation of ceramic pipe surfaces. Monthly evaluations of cooling coil loads emphasize the need for consistent system performance monitoring. Optimizing cooling pad thickness can reduce cooling coil load by 29.6%. A triangular design achieves a saturation efficiency of 95%, and mats made from coconut and banana fibers enhance saturation effectiveness. Increasing air intake velocity improves wet bulb efficiency, especially at higher temperatures. The research underscores the pivotal role of relative humidity, showing its impact on chilling capacity. These insights are crucial for designing and implementing semi-evaporative cooling systems in real-world scenarios, offering valuable guidance for system design, operation, and material selection.

Cite this article as: Javanjal VK, Gadhave S, Patil LN, Mahajan KA, Jadhav SS. Efficiency improvement of semi-evaporative cooling systems through environmental analysis. Sigma J Eng Nat Sci 2025;43(4):1113–1123.

INTRODUCTION

Evaporative cooling was used to preserve a pleasant climate inside historic buildings. There are benefits and drawbacks associated with the use of this methodology. It offers other benefits in addition to enhancing indoor air quality, lowering environmental impact, using less energy, being easy to use, and requiring less upkeep. In order for an evaporative refrigerator to function, thermal energy in the air must be changed from an observable to

an imperceptible or difficult-to-distinguish condition. The temperature and partial pressure differential between vapour and air cause the transfer of mass and heat. Vapor compression refrigeration, which uses CFCs or HCFCs, has a far worse environmental effect than evaporative cooling. Evaporative refrigerators use a lot less energy than electric vapor compression refrigeration systems for the transportation of water and air [1, 2]. The main drawback of evaporative coolers is that they need outside air to function.

*Corresponding author.

*E-mail address: subhash.gadhave534@gmail.com

This paper was recommended for publication in revised form by Editor-in-Chief Ahmet Selim Dalkilic



The temperature differential that occurs between the moist and dry bulbs causes evaporation [3]. Evaporative cooling systems come in a variety of configurations and may be divided into three main categories: indirect, direct, or semi-indirect [4]. High temperatures and dry weather are ideal settings for evaporative coolers to operate in. There are several different types of climates in India, such as hot and dry, cold, warm and humid, temperate, composite, and tropical. There is a wide range of warm-humid, hot-dry, and variable climates. Direct evaporative coolers lose efficiency in warm, humid locations from 80% to 90% relative humidity (RH) in the summer. Because of the relatively low humidity levels in this area, which range from 30% to 50%, direct evaporative coolers are often used. Refrigerators that use direct evaporation simplify the process of controlling humidity and temperature [5,6]. Meanwhile, academic research indicates that the creation of an indirect evaporative chiller that is both flexible and energy-efficient is about to happen. Compared to traditional refrigeration techniques, indirect evaporative coolers have less pollution and better environmental benefits. It has been shown that evaporative coolers may save energy in dry and hot climates all over the world. The evaporative chiller system is in charge of providing comfort inside the building [1, 2, 4, 7-10]. Researchers have previously looked at the thermodynamics of evaporative coolers and ways to increase the efficiency of direct and indirect designs by using tubing and plates. The possible advantages of heat pipes, dew points, and semi-indirect evaporative cooling techniques have not been thoroughly studied. To fully understand the mass and heat transport processes inside these innovative evaporative cooler systems, further theoretical and empirical study is needed [1, 11]. Heat transmission devices with high efficiency are known as heat pipes. It has the ability to transport heat without the need for more energy [12]. Heat recovery heat pipes are a common kind of heat exchanger in HVAC systems. Wang et al. [13] achieved secondary heat recovery by including a heat pipe heat exchanger (HPHE) in their HVAC system. Ragil et al. [14] created a high-performance heat exchanger (HPHE) specifically with the aim of providing HVAC systems for hospital isolation chambers that are used to treat patients with respiratory diseases. The feasibility of installing vertical U-shaped fins on a high-performance heat exchanger (HPHE) to reduce the energy consumption of HVAC systems used for cooling and reheating purposes was investigated by Hakim et al. [15]. FJR Martinez et al.'s 2003 research [16] focused on heat ducts and evaporative coolers. Implementing a mixed-air energy recovery system is the main goal of this project, which aims to enhance indoor air quality. The results show that by using the energy from air circulation, air conditioning systems that include an air recovery system—which consists of heat pipes and an indirect evaporative cooler—may become more energy efficient. Liu Y. and colleagues used elevation refrigerators for their heat pipeline research. The hybrid cooling system's efficiency

is greatly increased by dew point evaporative chillers and microchannel heat pipes [17]. There is a dearth of studies on the use of finned heat ducts in evaporative coolers. Riffat et al. [18] first documented the use of heat pipes in evaporative refrigerators in 2004. Later writers carried on the research [19–21]. Global power costs have surged as a result of growing demand from the commercial and industrial sectors. Saudi Arabian electricity is costly, and freezers use a significant amount of energy from the power system [22–25]. Evaporative cooling (EC) is a very cost-effective and efficient way to reduce the energy required for space cooling by using a VCR system. Because the water pump and compressor have lower power outputs than the VCR system, the EC system uses less energy. When compared to a VCR system, the costs of setting up, maintaining, and running an EC system are lower [26–28]. As air moves over the cooling mats, water takes up heat from the surrounding atmosphere, lowering the overall air temperature. Higher dry bulb temperatures and lower relative humidity all help to improve EC cooling efficiency. Scientists have studied the EC system in great detail to increase its efficacy. An evaporative cooling (EC) system's performance is affected by a number of factors, such as air flow rate, ambient air conditions (such as humidity and temperature of the dry bulb), and the flow rate, thickness, density, and substance of the cooling pad water [29–34].

EXPERIMENTAL PROCEDURE

System of Cooling

Thermoelectric coolers, vapor compression chillers, vacuum coolers, and compressor-determined metal hydride cooling systems are examples of electrically powered cooling equipment.

The most powerful electrical system is found in the air conditioning Vapor Compression Chiller (VCC). Although the compressor-driven metal hydride cooling system has been studied in the literature, this is just the initial stage. Thermoelectric coolers have a wide range of uses, including medical, communications, military, and vacuum food coolers.

Compressor-Driven Metal Hydride Cooling (CDMHC)

The Compressor-Driven Metal Hydride Cooling (CDMHC) is an environmentally friendly hydrogen absorption and release system. A compressor creates a pressure difference between two metal reactors to desorb H₂. The biggest disadvantage of the method is the removal of parasites. Because parasite wounds are reduced in the CDMHC, its COP may be higher than in the VCC. In metal hydride cooling systems powered by compressors, unexpected load changes and startup have less of an influence on compressor overloading [30]. Mazumdar et al. [32], [33], [34], and Park et al. [31] evaluated CDMHC's cooling capacity and unique potential to increase performance. They observed

that the characteristics of metal hydrides had a significant influence on structural efficacy. Improvements in compressor efficiency, metal conductivity, slurry mass ratio, and compressor pressure ratio in the direction of hydrogen enhance the coefficient of performance (COP).

Cooling By Thermodynamics

To link the system with the sorption structures, the sorption technique and ejector cooling are utilized. Chemical or physical sorption brings one substance near another. The most common thermally powered sorption devices for HVAC in buildings are adsorption, absorption, and desiccant dehumidifiers. Sorption may also be utilized to cool hot metal hydrides.

Cooling Based on Absorption

This theory is based on the fact that liquids may both desorb and absorb vapor from another fluid, the solubility of which varies with pressure and temperature. The condenser cools the superheated vapor structure of the refrigerant that the generator generates when the force is high. As the condensed refrigerant evaporates at low pressure, the intermediate temperature falls. At this time, the vapor from the evaporator escapes with a spray of the weak refrigerant solution over the top of the absorber. The heat is delivered to the cooling fluid from the condenser and absorber. For the most part, the only alternatives are H₂O and NH₃, or LiBr and H₂O. A rectifier is necessary when utilizing H₂O/NH₃ as an absorbent in an absorption cooling system to eliminate the water before the NH₃ reaches the condenser.

Efficiency Variations Caused By Semi-Direct Evaporation

The outside air temperature, air intake velocity effects and their configurations, cooling pad thickness, cooling capacity, and saturation competence affect a semi-indirect evaporative cooling system's thermodynamic performance. A modification in the configuration of the cooling medium concludes the behavior pattern of the semi-indirect evaporative cooling system. This study goes far beyond just suggesting that asymmetrical cooling pads provide remarkable performance. This information contrasts the thermodynamic research configurations on the structure's three sides, employing square, hexagonal, pentagonal, octagonal, and triangular patterns and shapes to make use of the cooling medium's wetted surface area in semi-indirect evaporative cooling.

COOLING ANALYSIS

Experimental Cooling Pad Analyses

In typical air conditioners, the cooling coil and condenser work together to offer the most efficient cooling pads. The LMTD (Logarithmic Mean Temperature Difference) model is used to estimate the effectiveness of cooling pads. This follow-up research phase's objective is to finally get there. We'll look at the distinctions between buildup cooling pads and conservative cooling pads in this section.

Some study investigates the possibilities of a cooling pad to decrease agricultural waste. Sugar cane, banana tree, coconut, honeycomb paper, and khus fibers are employed in this inquiry. The packing density for all four cooling pads is 44.44 kg/m³. The honeycomb paper pad was incised to the same size as the extra build-up cooling pads using a 90° tumbler method. New vendors' khus fibers, honeycomb fibers, coconut fibers, and even sugarcane and banana fibers may be subjected to lab testing with unpredictable airflow.

It is detailed how the experimental setting for analyzing five different kinds of cooling pads was created. Because bananas, coconut fibers, and sugarcane are considered agricultural waste, they are available all year in India.

Experiment Parameters

Because of human mistakes; physical and technical limits, every inquiry has some positive uncertainty and error. The consequences of such autonomous imprecision are highly debated. The approach described here investigated factors such as air velocity, relative humidity, and temperature. Table 1 highlights details on the instruments, as well as parameters.

Processing Thermocouple Application

The utilization of measuring tools, techniques, and standards is required for thermocouple calibration. Before using a thermocouple, the temperature must be set such that it stays consistent across a suitably large region. Thermostatic reference points that can be adjusted A graphite thermometer acts as a fixed-point unit in a graphite crucible holding a metal component. When it freezes, this metal component maintains a somewhat steady temperature. A simple calibration procedure requires just a few instructions. To do a basic calibration, water is heated to 30 degrees. The open end of the thermocouple is then connected to both multimeters, and since both ends of the thermocouple are at

Table 1. Details on the instruments, as well as parameters

Parameter	Instruments	Accuracy	Range
Air volume	Air flow meter	±3%	40 to 4000 m ³ /h
Relative humidity/ dry bulb temperature	Thermograph	±3%/±0.5°C	0 to 100%/ 0–100°C
Vane anemometer	Air velocity	±(0.2 m/s+2%)	0.4 to 20.0 m/s

the same temperature, the device multimeter must read 0 microvolts. The power is shown after the multimeter measurement is constant. Voltage measurements are obtained once again at 37 degrees Celsius. This procedure of increasing the temperature by 5 degrees Celsius is repeated until the temperature reaches 60 degrees Celsius.

Revolutionizing Cooling Systems

In a semi-indirect evaporative cooling system with two independent airstreams, rock-solid absorbent ceramic pipes allow for mass transfer as well as heat transmission. This is a revolutionary strategy since the pipes filter out germs and inhibit the spread of legionella. This set-up is called a semi-indirect evaporative cooling system because the main airstream's specific humidity depends on mass transfer, heat (mass transfer) depends on humidity, and the porous pipe's ability to let more or less water pass through it. The building's improvement diversion arrangement defines the room's bounds. This semi-indirect evaporative cooler (SIEC) uses two different air streams, one for chilling and one for making indirect contact with water, to increase evaporative cooling efficiency. Water is recycled with the expelled air because it is vital. T5 equals 400°C, T4 equals 36.50°C, T3 equals 330°C, T2 equals 29.50°C, and T1 equals 260°C temperature was selected.

RESULTS AND DISCUSSION

Figure 1 shows how the variable confirmation air pace affects product air temperature and wet bulb efficiency. This illustration also compares the velocities and efficiency of the intake air channels. The air temperature in the two channels is between 30 and 35 degrees Celsius, the humidity is 35% (the wet bulb temperature ranges between 18.9 and 23 degrees Celsius), and the air velocity ranges between 3 and 2.5 meters per second (m/s), 2 and 1.5 meters per second (m/s), and 1 meter per second (m/s). The wet bulb efficiency of mutually negative air heat decreased from 1 to 2 m/s. The air velocity was confirmed to be 1-2 meters per second, and the wet-bulb efficiency for heating the air between 30 and 35 degrees Celsius made sense.

Wet bulbs may have an efficiency of more than 100% when the air rate for directly heated air is less than 2 m/s. While the air temperature increased linearly with the confirmed air rate for both the 35oC and 30oC delta temperatures, the dew point temperature may have been refined within that cooler at velocities less than 2 m/s. The functional air rate is enhanced to achieve the condensed abruptness consumed by operational air in a wet channel, which causes contact with the operational air and minimizes the wet exterior. In order to minimize the focus on air temperature for input air temperatures below their wet-bulb efficiency and wet-bulb temperature of more than 100%, the cooler's speed should be between 1 and 2 meters per second.

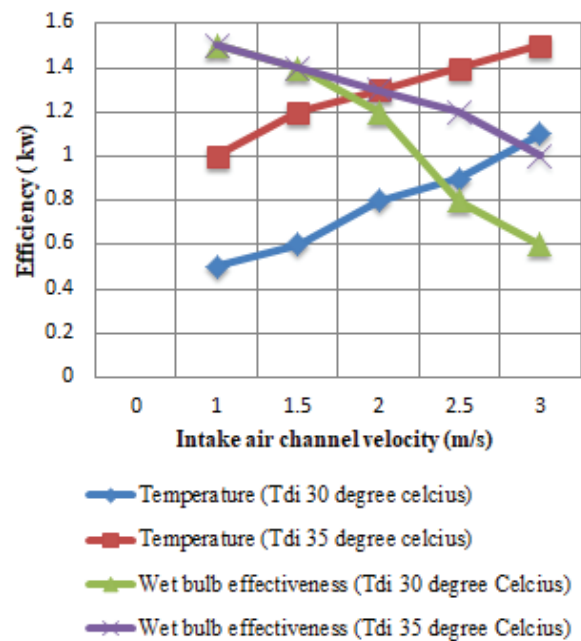


Figure 1. Efficiency and intake air channel velocity comparison.

Intake Channel Impact Humidity

The measured effects of inlet relative humidity and access air rate on water consumption are shown in Figure 2. The input air channel velocity and water use are compared in this scenario. The relative humidity of the incoming air may be between 55% and 45% at 35 degrees Celsius and 1-2 meters per second.

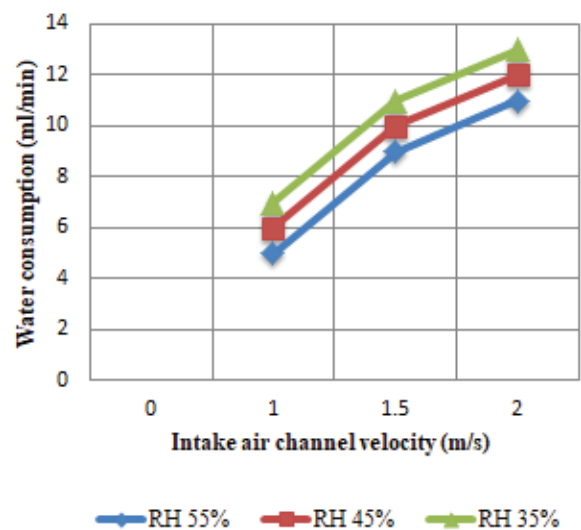


Figure 2. Water usage and intake air channel velocity are compared.

Efficiency of Temperature Regulation

If you put 35°C air into a dry channel with 35% relative humidity (dew point 17.9°C, wet bulb temperature, and Twb 23°C), Figure 3 shows the temperature, relative humidity, and mass flood percentage of the air that comes out. Figure 4 shows comparison of the amount of water used and the speed of the intake air path.

Wet Bulb Efficiency, Dew Point, Dew Point Temperature, Coefficient of Performance, and Relative Humidity

Figure 5 demonstrate the effects of adjusting the relative humidity of the intake air on cooling capacity, COP, dew point, and wet bulb efficacy. The supply air flow rate was 0.0032 kg/s, the input air temperature was 35 °C, and the relative humidity levels were 55, 50, 45, 40, and 35%, respectively. A positive relationship occurs between relative humidity, cooling capacity, and COP, whereas a negative relationship exists between several quantities. More humid incoming air benefits both the cooling capacity and the COP of the structure. Because the vapor force separation between the air and water borders is more prominent when the intake air humidity is low, even if the inlet air humidity is low, more wetness will be brought in via the wet channel. Figure 6 shows comparison between cooling unit and power usage.

Strong Action

This study made no mention of a structure built to regulate its cooling load and vapor density, aiming for COP 3. The total power consumption of the two cooler types is shown in Figure 6. If the evaporative cooling structure association is implemented, the lattice top power requirements might be lowered by 163 MW. Running the evaporative cooling units beyond the excursion hour is anticipated to

cost SAR 1.06 million, or nearly the same as the electricity excise charge of 0.175 SAR/kWh. The electrical expenses for operating the air-shaping vapor density structure at the same time would be more than SAR 5 million to SAR 5.25 million. The energy expenses of operating an evaporative cooler are often lowered by more than 70%.

As seen in Figure 7, all of the cost structures and COPs are well-known. Evaporative cooling systems reduce both electricity consumption and greenhouse gas emissions while also providing a nice breeze. Based on the discharge

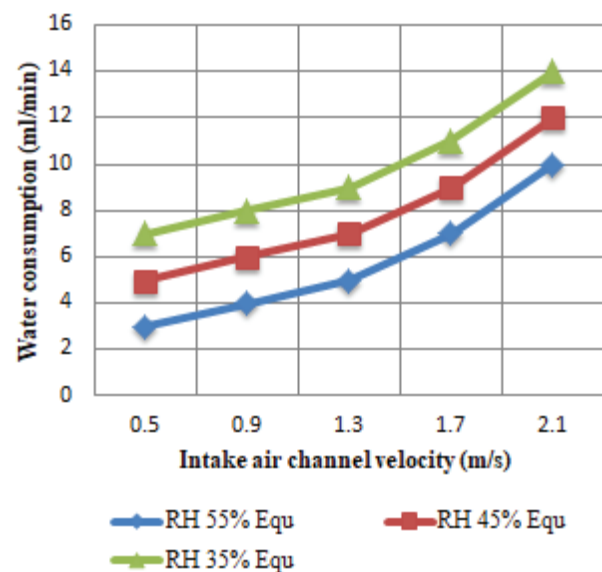


Figure 4. Comparison of the amount of water used and the speed of the intake air path.

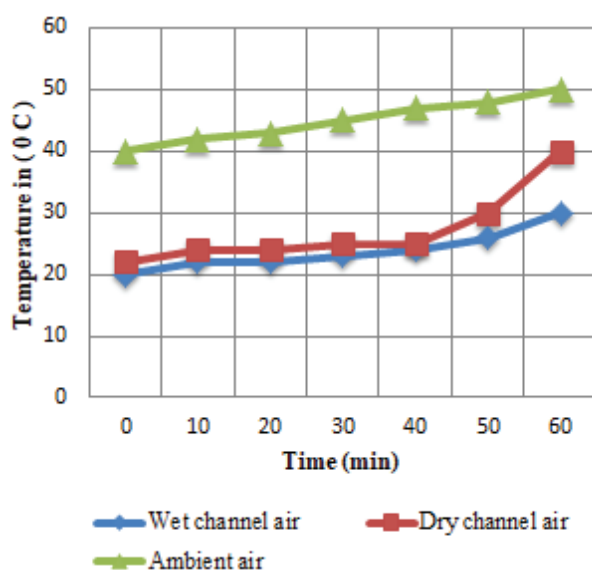


Figure 3. Temperature and time series comparison.

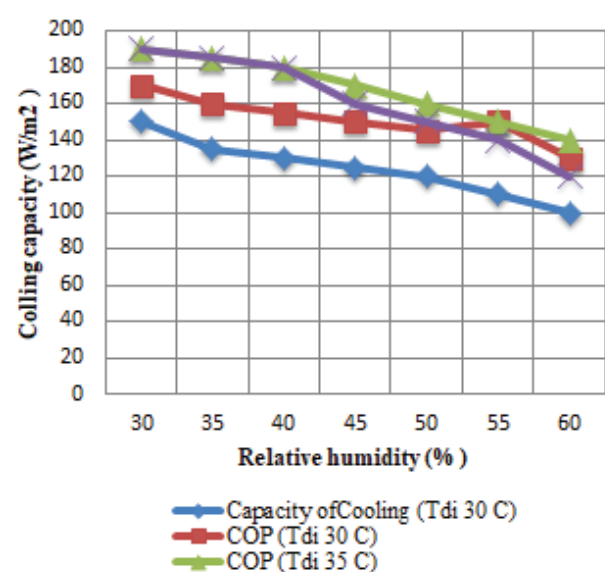


Figure 5. Compared cooling capacity and relative humidity.

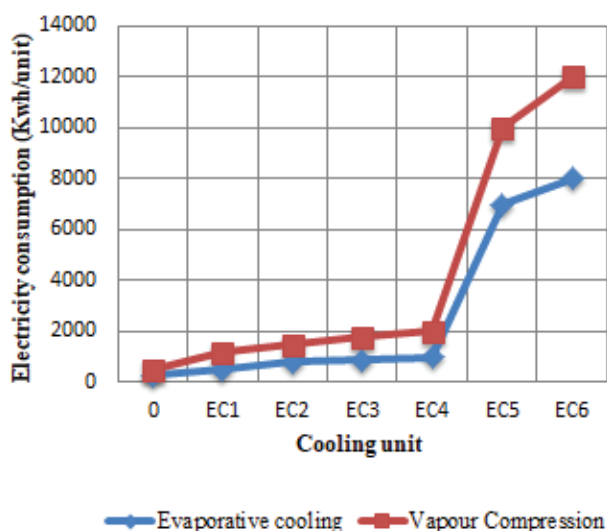


Figure 6. Comparison between cooling unit and power usage.

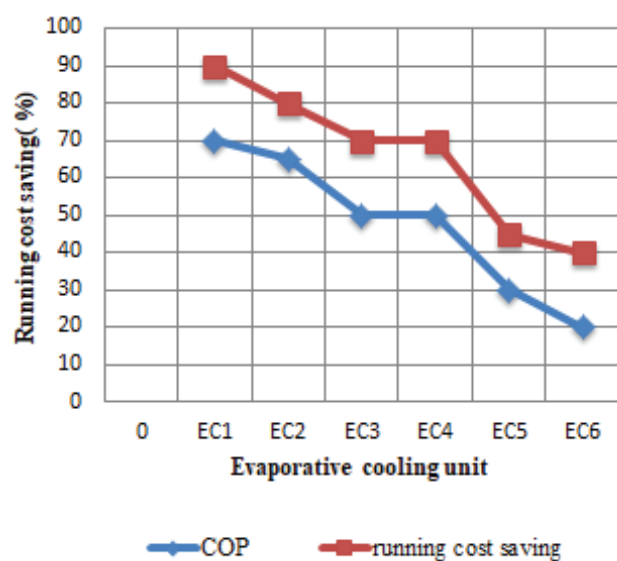


Figure 7. Comparison of an evaporative cooling system and an operating cost-saving option.

aspect of the power age mix of 0.75kg CO₂ l/kWh, vapor compression systems and evaporative cooling structures save 24600 tons of CO₂ (a 78% savings). The percentage reduction in CO₂ emissions obtained by each evaporative cooler is shown. Figure 8 shows comparison of temperature and sensible heat recovered.

Table 2 contains the complete ANOVA breakdown. The relationships between volumetric flow rate (VxT), temperature (HLxT), and relative humidity (VxHL) are shown in the first section. Part 2 displays the sum of squares (SS)

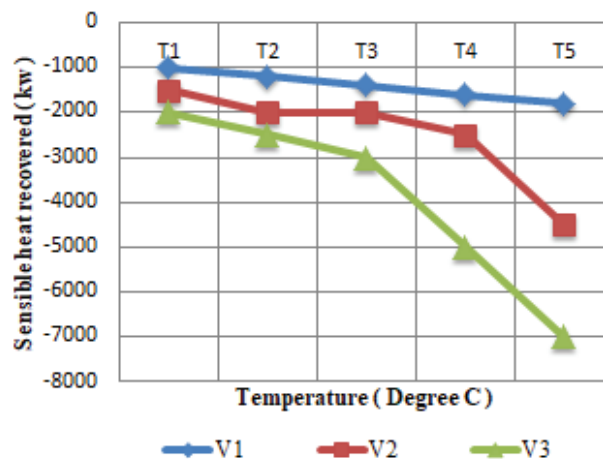


Figure 8. Comparison of temperature and sensible heat recovered.

Table 2. Analysis of variance for enhanced sensible heat

Factors	SS	Dof	%	V
HL	4047449	3	5.85	3215646
V	10580562	3	13.45	6482202
T	10478477	5	13.35	3842907
HLxT	11732658	9	14.75	2705554
VxT	39192291	9	46.35	6138008
VxHL	3675375	5	5.45	2142132
Error	7926067	17	10.35	1742193
Total	86880071	45	100	3226351

for each angle. The DoF of the investigated variables is displayed in segment 3, followed by the percentage of variation explained in segment 4, and lastly the variance values in segment 5. These are the most tense results from these investigations.

Air Flow Analysis

The usual velocity contribution is close to 12%, according to Table 2. An increase in the convection coefficient of the outer stream results in an increase in air stream power.

Temperature Analysis

The rate of heat transfer determines whether or not heat exchangers are used to separate temperatures. When the temperature difference between the outside and recirculated air streams widens, rationality heat rises. At 12%, responsibility for variance analysis is rather close (Table 2).

VxT

Table 2 shows the greatest contributing velocity using a 45% inference. The entity aspect is supported via aspect rejection cooperation. In response to increasing

temperatures and airflow, rational heat is increased, and stage and upright progress. The findings are consistent and predictable. Practical expertise with danger assessment improves heat recovery. As a result, the V5 and T3 are the most cost-effective solutions.

HLxT

Table 2 shows a median contribution rate of 13%. The greatest practical rise in heat is associated with the highest temperature and average relative humidity. The close closeness of the humidity stages for each temperature determined accounts for the moisture specific aspect's low responsibility.

Error

This demonstrates the larger degree of contribution, with a 9% inaccuracy vs a 4.5% error attributable to humidity. Examining the VxHLxT triangle connected with this rate could help us find out.

Enhancement of Infrared Heat

The ANOVA results are shown in Table 3. The variables that were studied are shown in Section 1: humidity, velocity, and the correlations between humidity and temperature (HLxT), velocity (VxT), and temperature (VxHL). The second portion is the aspect's sum of squares (SS).

Table 3. Latent heat variation analysis

Factor	V	SS	Dof	%
T	24098204	125534148	5	8.75
V	3556597	55901637	3	1.55
HL	279907892	575020867	3	39.25
VxT	28388298	230153496	9	16.05
HLxT	54301993	437463055	9	29.95
VxHL	14852220	68550215	5	4.85
Error	8252382	122896783	17	8.55
Total	34984267	1487506877	33462307	101.25

Table 4. Analysis of variance for enhanced total heat

Factors	V	SS	DoF	%
HL	252698197	517584838	3	41.25
V	27230791	66650026	3	5.35
T	62711217	266019481	5	21.25
HLxT	27760882	225134172	9	17.95
VxHL	14807536	68371478	5	5.45
VxT	11017640	91188231	9	7.35
Error	8478385	126512835	17	10.15
Total	30042014	1270047737	45	100

Examining The Humidity

The causal velocity of 38% given in Table 4 is the highest for that component. When the humidity in a pipe is low, water evaporates from its surface. This increased humidity may prevent dehumidification, which is associated with depressing latent heat, resulting in a reduction in pleasant moisture.

VxT

Table 3 displays the total speeds of all key components at 15% closure. The extraordinary dehumidification impact (mean values dropping) and proximity values explain the zero dependability of the distinctive features. Table 3 of HLxT shows a 29% similarity to the causal velocity. HLxT enables users to zero in on a single query. When the air is hot and dry, a lot of water evaporates, but when the humidity is high, the detailed humidity value is high, and the conditions for pipe reduction are ideal. Even if the humidity level is lower, the same rationale may apply to rapid temperature readings. Static heat exchange is decreased in this manner.

Temperature Increase

The Analyses of Variance for enhanced total heat are shown Table 4. The many components that are meant to indicate degree-enhanced heat.

In terms of the variance investigation, HLxT is the most causative. The ANOVA findings are shown in Table 4. Section 1 depicts the separation of relative humidity, volumetric flow velocity, and their associated temperature x-relationships (HLxT, VxT, and VxHL). The variance values in segment 2 are V-connected. Section 3 displays the sum of squares (SS) of the components; Section 4 displays their degree of freedom (Dof); and Section 5 displays their relative velocities (%).

Temperature

This is considerable, even when just a minor quantity of heat recovery is used. Because of the combined impacts of both the rational and torpid heat special effects, higher temperatures have a negative influence on the overall indicate value. The humidity relative This accounts for the lion's share of the 40%. This is the fundamental concept of passive heat supply. Because of the connection of instantaneous rational heat recuperation, the SIEC is advantageous to indirect evaporative cooling structures, but mass transfer marvels have needed more sensible heat.

HLxT

The HL1 (low humidity level) indicates that sensible and passive heat recovery should be avoided in general. This picture changes when relative humidity goes up, especially at the highest temperatures (T5, T4, and T3), where latent and rational heat are both negative and condensation happens, supporting the tilt seen in the single feature. Experiments were carried out in order to improve the presentation of the fiber-tube evaporative air cooler. We evaluated a variety of

humidity levels, input temperatures, and flow speeds. These include operating the system dry initially, then with water to imitate condensation on the cooler's fiber tubes. Primary (for system operation) and secondary (for system output) air often enter the system via the same ports. A variable air stream's impact velocity was also observed. The outcomes of the experiments in different contexts are explained in Table 5.

The Test Run

For this test, the evaporative cooling surface of the fibers was not moist. It provided a horizontal supply strategy for determining the evaporative cooling capability of wet fiber material. The temperature variations throughout the presentations were minor, suggesting that the cooling effect was limited.

RH_{in}: Inlet relative humidity at ambient temperature; T_{in}: Set ambient inlet temperature; T_{dry_out}: The

temperature of the dry air channel from the exit (product or supply air); T_{wet_out}: The temperature of the wet air channel at the outflow (process or working air); RH_{dry_out}: The relative humidity of the dry air channel at the output; RH_{wet_out}: The relative humidity from the wet air channel to the output.

System Efficiency and Water Usage Velocity

The system efficiency and water utilization concerns were resolved at the highest input dry bulb temperature, as shown in Table 6. Because the essential framework's indirect mode of operation functions in many environmental situations, including the analysis of the heated feasibility linked with the adiabatic immersion temperature, a precedent mechanism on the cooling rise must be constructed. Warm ampleness estimates are equivalent for similar outside cools.

Table 5. Results of the dry test scenario in terms of relative humidity and temperature (only for un-wetted evaporative cooling surface)

T _{in} (°C)	RH _{in} (%)	T _{wet_out} (°C)	T _{dry_out} (°C)	RH _{wet_out} (%)	RH _{dry_out} (%)
22.3	40.1	22.3	21.8	44.1	42.3
22.3	40.1	22.3	21.8	44	42.2
22.4	40.1	22.3	21.8	44.3	42.3
22.4	40.1	22.3	21.8	44.1	42.2
22.5	40.3	22.3	21.8	44.1	42.2
22.6	39.7	22.3	21.8	44.1	42.1
22.7	40.6	22.3	21.8	44	42.2
22.7	39.6	22.3	21.8	43.9	42.3
22.7	39.6	2.2	21.8	44.2	42.2
22.7	39.6	22.2	21.8	44.1	42.2
22.6	39.7	22.3	21.8	44.1	42.1

Table 6. Test for inlet dry bulb temperature

Air Flow Channel	RH outlet (%)	T outlet (°C)	RH inlet (%)	T inlet (C)
Process or wet air	88.5	23.2	10.2	41.4
Supply or dry air	53.5	22.2	10.2	41.4

Table 7. Variations in the tabular layout of cooling load savings

S. No	T _{ci} (°C)	Saving In Q _{ci} (%)	T _{cii} (°C)	Q _{ci} (kJ/s)	Q _{cii} (kJ/s)	Mai (kg/s)	Q _{sr}	Maii	Months
1	19	64.43	3.33	2.73	5.31	1.59	2.06	1.36	March
2	19	29.373	3.33	4.83	6.24	1.59	1.94	1.36	April
3	19	27.9	3.33	4.94	6.29	1.6	1.92	1.36	May
4	19	-51.98	3.33	11.93	8.22	1.63	1.74	1.36	June

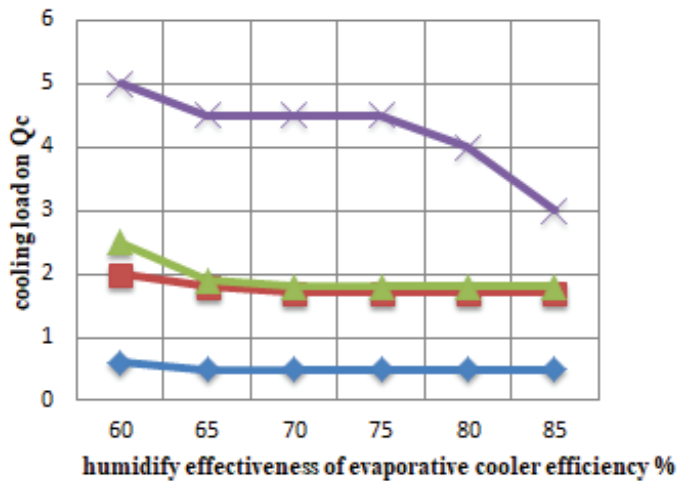
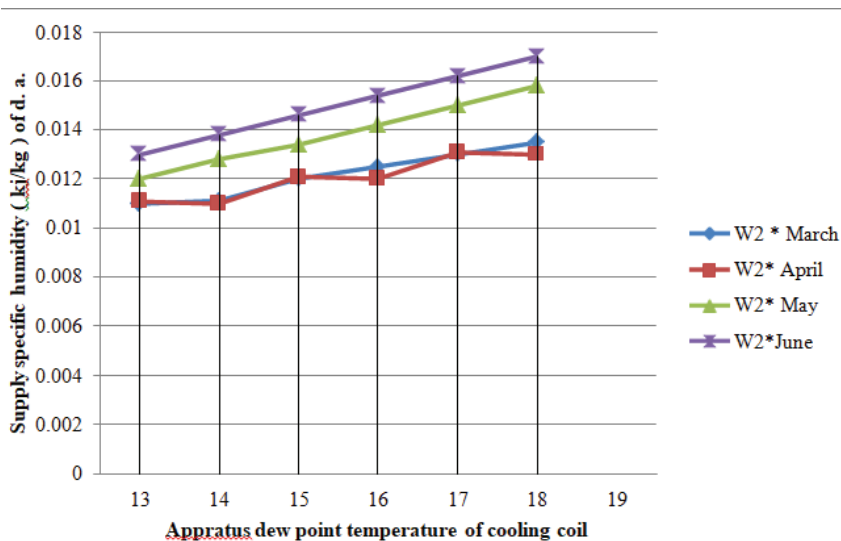
Table 8. Deviation in the cooling coil's load during cooling

S. No	Tci ((°C))	Qci (kj/s)	Qsr (Kj/s)	Efficiency (%)	Mai (Kg/s)	(X)	Months
1	19	0.76	1.025	71.235	0.365	0.435	March
2	19	1.585	1.025	71.235	0.375	0.435	April
3	19	1.709	1.025	71.235	0.385	0.435	May
4	19	4.258	1.025	71.235	0.395	0.435	June

Ceramic evaporative systems are less visible than other kinds of water purification systems due to their dependency on the water route during the susceptible exterior's porous conditions and smoke phobia. In terms of monthly variable cooling loads, compare the semi-evaporative cooling system with the ceramic pipe redesign to the traditional

cooling system and tables 7 for basic construction. Table 8 shows a monthly breakdown of the load of cooling on cooling twist with respect to different factors.

In our test setup, an assortment of cooling events occurred on the cooling coil to humidify within the enhanced semi-evaporative cooling system as per the

**Figure 9.** Comparison of the humidifier's efficacy and the coil's cooling load for evaporative coolers.**Figure 10.** Comparison of the apparatus's dew point temperature and supply specific humidity.

supplied limit as shown in Figure 9. Further, comparison of the apparatus's dew point temperature and supply specific humidity is mentioned in Figure 10.

CONCLUSION

When the air supply is near the ground and temperatures and relative humidity are high, the model predicts that the ceramic pipe surface will evaporate. Each month, the cooling coil loads of semi-evaporative cooling versus traditional air conditioning were evaluated.

- The wet-bulb efficiency is around average at 2 meters per second of intake air velocity.
- Reduced relative humidity leads to a reduction in chilling capacity. When the relative humidity exceeds 55%, the wet bulb effect becomes 21% more intense than the dew point effect.
- The effectiveness of the wet bulb is increased by increasing the velocity at which air enters it. When the input air velocity is 2.5 m/s, the effectiveness of wet bulbs at 35°C T_{di} is increased by 26.2%.
- A range of parameters, including ventilation, temperature, and relative humidity, were taken into account when considering both sensible and latent heat enhancement. Three interdependent variables must be in balance in the context of refrigeration: air temperature, air velocity, and dry-bulb air temperature.

AUTHORSHIP CONTRIBUTIONS

Authors equally contributed to this work.

DATA AVAILABILITY STATEMENT

The authors confirm that the data that supports the findings of this study are available within the article. Raw data that support the finding of this study are available from the corresponding author, upon reasonable request.

CONFLICT OF INTEREST

The author declared no potential conflicts of interest with respect to the research, authorship, and/or publication of this article.

ETHICS

There are no ethical issues with the publication of this manuscript.

STATEMENT ON THE USE OF ARTIFICIAL INTELLIGENCE

Artificial intelligence was not used in the preparation of the article.

REFERENCES

- [1] Xuan Y, Xiao F, Niu X, Huang X, Wang S. Research and applications of evaporative cooling in China: a review (II)—systems and equipment. *Renew Sustain Energy Rev* 2012;16:3523–3534. [\[CrossRef\]](#)
- [2] Kowalski P, Kwiecien D. Evaluation of simple evaporative cooling systems in an industrial building in Poland. *J Build Eng* 2020;32:101555. [\[CrossRef\]](#)
- [3] Duan Z, Zhan C, Zhang X, Mustafa M, Zhao X, Alimohammadisagvand B, Hasan A. Indirect evaporative cooling: past, present and future potentials. *Renew Sustain Energy Rev* 2012;16:6823–6850. [\[CrossRef\]](#)
- [4] Xuan Y, Xiao F, Niu XF, Huang X, Wang SW. Research and application of evaporative cooling in China: a review (I)—Research. *Renew Sustain Energy Rev* 2012;16:3535–3546. [\[CrossRef\]](#)
- [5] Bishoyi D, Sudhakar K. Experimental performance of a direct evaporative cooler in composite climate of India. *Energy Build* 2017;153:190–200. [\[CrossRef\]](#)
- [6] Porumb B, Ungureşan P, Tutunaru LE, Şerban A, Bălan M. A review of indirect evaporative cooling operating conditions and performances. *Energy Proc* 2016;85:452–460. [\[CrossRef\]](#)
- [7] Guan L, Bennett M, Bell J. Evaluating the potential use of direct evaporative cooling in Australia. *Energy Build* 2015;108:185–194. [\[CrossRef\]](#)
- [8] Baakeem SS, Orfi J, Bessadok-Jemai A. Thermodynamic and economic analysis of the performance of a direct evaporative cooler working under extreme summer weather conditions. *J Mech Sci Technol* 2018;32:1815–1825. [\[CrossRef\]](#)
- [9] Bom GJ. Evaporative air-conditioning: Applications for environmentally friendly cooling. World Bank Publications; 1999. [\[CrossRef\]](#)
- [10] Smith ST, Hanby VI, Harpham C. A probabilistic analysis of the future potential of evaporative cooling systems in a temperate climate. *Energy Build* 2011;43:507–516. [\[CrossRef\]](#)
- [11] Sajjad U, Abbas N, Hamid K, Abbas S, Hussain I, Ammar SM, Sultan M, Ali HM, Hussain M, Wang CC. A review of recent advances in indirect evaporative cooling technology. *Int Commun Heat Mass Trans* 2021;122:105140. [\[CrossRef\]](#)
- [12] Putra N, Ariantara B. Electric motor thermal management system using L-shaped flat heat pipes. *Appl Therm Eng* 2017;126:1156–1163. [\[CrossRef\]](#)
- [13] Wang H, Zhou S, Wei Z, Wang R. A study of secondary heat recovery efficiency of a heat pipe heat exchanger air conditioning system. *Energy Build* 2016;133:206–216. [\[CrossRef\]](#)
- [14] Sukarno R, Putra N, Hakim II, Rachman FF, Mahlia TMI. Utilizing heat pipe heat exchanger to reduce the energy consumption of airborne infection isolation hospital room HVAC system. *J Build Eng* 2021;35:102116. [\[CrossRef\]](#)

- [15] Hakim II, Sukarno R, Putra N. Utilization of U-shaped finned heat pipe heat exchanger in energy-efficient HVAC systems. *Therm Sci Eng Prog* 2021;25:100984. [\[CrossRef\]](#)
- [16] Martínez FJR, Plasencia MAA-G, Gómez EV, Díez FV, Martín RH. Design and experimental study of a mixed energy recovery system, heat pipes and indirect evaporative equipment for air conditioning. *Energy Build* 2003;35:1021–1030. [\[CrossRef\]](#)
- [17] Liu Y, Yang X, Li J, Zhao X. Energy savings of hybrid dew-point evaporative cooler and micro-channel separated heat pipe cooling systems for computer data centers. *Energy* 2018;163:629–640. [\[CrossRef\]](#)
- [18] Riffat SB, Zhu J. Mathematical model of indirect evaporative cooler using porous ceramic and heat pipe. *Appl Therm Eng* 2004;24:457–470. [\[CrossRef\]](#)
- [19] Alharbi A, Almaneea A, Boukhanouf R. Integrated hollow porous ceramic cuboids-finned heat pipes evaporative cooling system: numerical modeling and experimental validation. *Energy Build* 2019;196:61–70. [\[CrossRef\]](#)
- [20] Boukhanouf R, Amer O, Ibrahim H, Calautit J. Design and performance analysis of a regenerative evaporative cooler for cooling of buildings in arid climates. *Build Environ* 2018;142:1–10. [\[CrossRef\]](#)
- [21] Boukhanouf R, Alharbi A, Amer O, Ibrahim H. Experimental and numerical study of a heat pipe based indirect porous ceramic evaporative cooler. *Int J Environ Sustain Dev* 2015;6:104. [\[CrossRef\]](#)
- [22] Felimban A, Prieto A, Knaack U, Klein T, Qaffas Y. Assessment of the current energy consumption of residential buildings in Jeddah, Saudi Arabia. *Buildings* 2019;9:163. [\[CrossRef\]](#)
- [23] Almasri RA, Almarshoud AF, Omar HM, Esmaeil KK, Alshitawi M. Exergy and economic analysis of energy consumption in the residential sector of the Qassim region in the Kingdom of Saudi Arabia. *Sustainability* 2020;12:1–20. [\[CrossRef\]](#)
- [24] Al-Sulaiman FA, Zubair SM. A survey of energy consumption and failure patterns of residential air-conditioning units in eastern Saudi Arabia. *Energy* 1996;21:967–975. [\[CrossRef\]](#)
- [25] Yang X, Wang X, Liu Z, Luo X, Yan J. Effect of fin number on the melting phase change in a horizontal finned shell-and-tube thermal energy storage unit. *Sol Energy Mater Sol Cells* 2022;236:111527. [\[CrossRef\]](#)
- [26] Sawant AP, Agrawal N, Nanda P. Performance assessment of an evaporative cooling-assisted window air conditioner. *Int J Low Carbon Technol* 2012;7:128–136. [\[CrossRef\]](#)
- [27] Guo J, Liu Z, Yang B, Yang X, Yan J. Melting assessment on the angled fin design for a novel latent heat thermal energy storage tube. *Renew Energy* 2022;183:406–422. [\[CrossRef\]](#)
- [28] Guo J, Wang X, Yang B, Yang X, Li MJ. Thermal assessment on solid-liquid energy storage tube packed with non-uniform angled fins. *Sol Energy Mater Sol Cells* 2022;236:111526. [\[CrossRef\]](#)
- [29] Guo J, Du Z, Liu G, Yang X, Li MJ. Compression effect of metal foam on melting phase change in a shell-and-tube unit. *Appl Therm Eng* 2022;206:118124. [\[CrossRef\]](#)
- [30] Yang X, Guo J, Yang B, Cheng H, Wei P, He YL. Design of non-uniformly distributed annular fins for a shell-and-tube thermal energy storage unit. *Appl Energy* 2020;279:115772. [\[CrossRef\]](#)
- [31] Yan M, He S, Gao M, Xu M, Miao J, Huang X, et al. Comparative study on the cooling performance of evaporative cooling systems using seawater and freshwater. *Int J Refrig* 2021;121:23–32. [\[CrossRef\]](#)
- [32] Omidi Kashani B. Increase of energy efficiency ratio of a direct evaporative cooler by dynamic behavior with energy and exergy analysis. *Proc Inst Mech Eng Part C J Mech Eng Sci* 2022;236. [\[CrossRef\]](#)
- [33] Abaranji S, Panchabikesan K, Ramalingam V. Experimental investigation of a direct evaporative cooling system for year-round thermal management with solar-assisted dryer. *Int J Photoenergy* 2020;2020:698904. [\[CrossRef\]](#)
- [34] Almaneea A. Experimental and numerical investigation of single-phase forced convection in flat plate heat exchanger with different numbers of passes. *Arabian J Sci Eng* 2020;45:9769–9776. [\[CrossRef\]](#)